



# Simultaneous Detection of Glucose and Acetoacetate in Artificial Urine Samples Using 3D-Connector Microfluidic Paper Based Analytical Devices

Ahmad Luthfi Fahmi<sup>1</sup>, Kamila Rohadatul 'Aisy<sup>1</sup>, Ika Oktavia Wulandari<sup>1</sup>, Hermin Sulistyarti<sup>1</sup>, Akhmad Sabarudin<sup>1\*</sup>

<sup>1</sup>Department of Chemistry, Faculty of Science, Brawijaya University, Malang, Indonesia.

Received: May 29, 2024

Revised: September 18, 2024

Accepted: December 25, 2024

Published: December 31, 2024

Corresponding Author:

Akhmad Sabarudin

[sabarjpn@ub.ac.id](mailto:sabarjpn@ub.ac.id)

DOI: [10.29303/jppipa.v10i12.7825](https://doi.org/10.29303/jppipa.v10i12.7825)

© 2024 The Authors. This open access article is distributed under a (CC-BY License)



**Abstract:** Diabetic patients sometimes experience both hyperglycemia and hyperketonemia simultaneously. This condition requires proper management of glucose and ketone body biomarkers. The fluctuating intensity of these biomarkers necessitates regular monitoring. This study aims to develop concept non-enzymatic measurement method by integrating  $\mu$ PADs (microfluidic paper-based analytical devices) for detecting glucose and acetoacetate in artificial urine samples. The method uses silver nanoparticle formation for glucose detection and Schiff base reaction as well as the Rothera test for acetoacetate detection. Optimal conditions found include the glucose detection zone with volume ratio of  $\text{AgNO}_3$  500 mM : starch 3% (w/v) (1 : 1), and the acetoacetate detection zone with glycine 900 mM in phosphate buffer pH 9.4. The artificial urine sample combination consists of glucose, acetoacetate, and acetone with volume ratio of (1 : 1 : 1). The 3D-Connector for glucose uses NaOH 10 M : starch 3% (w/v) with volume ratio of (1 : 3), while for acetoacetate, sodium nitroprusside 15% (w/w) in DMF 5% (v/v). Validity for glucose measurement shows linearity ( $R^2 = 0.9664$ ), precision (RSD = 4.56%), accuracy (88.75 - 99.62%), LOD (1.61 mM), and LOQ (5.37 mM). Conversely, acetoacetate measurement shows linearity ( $R^2 = 0.9636$ ), precision (RSD = 1.24%), accuracy (99.44 - 99.73%), LOD (1.41 mM), and LOQ (4.69 mM).

**Keywords:** Biomarkers; Diabetes; Non-enzymatic; Paper-based devices

## Introduction

Glucose is the primary energy source that the body needs to fulfill its vital functions. The vital role of glucose in the body makes its imbalance detrimental to the overall functioning of cells. Deficiency of glucose levels in the blood can accelerate lipolysis and stimulate the liver to produce ketones. This condition may be beneficial in reducing body fat, but if fat breakdown is excessive, the body may experience hyperketonemia. Hyperketonemia is similar to hyperglycemia, which is indicated by high levels of ketones in the body. Individuals with hyperglycemia while fasting usually

have blood glucose levels higher than 125 mg/dL, whereas hyperketonemia occurs when blood ketone levels are in the range of 7-25 mmol/L (Hillock et al., 2024; Nasser et al., 2020; Ramteke et al., 2019). Elevated glucose and ketone levels can occur simultaneously in diabetic patients. Three significant factors that can trigger diabetes include genetic, metabolic, and environmental factors. Metabolic factors are a crucial issue that is often overlooked by many people, especially those who are obese, have low physical activity, and have an unhealthy diet (Galicía-García et al., 2020; Hassan et al., 2022). Preventive measures to address the elevation of both biomarkers involve controlling

## How to Cite:

Fahmi, A. L., 'Aisy, K. R., Wulandari, I. O., Sulistyarti, H., & Sabarudin, A. (2024). Simultaneous Detection of Glucose and Acetoacetate in Artificial Urine Samples Using 3D-Connector Microfluidic Paper Based Analytical Devices: English. *Jurnal Penelitian Pendidikan IPA*, 10(12), 10053–10064. <https://doi.org/10.29303/jppipa.v10i12.7825>

nutrient intake based on the results of body biomarker measurements. Common testing methods in circulation are known as invasive methods, involving the collection of skin, fluid, or internal body tissue samples. Invasive methods tend to be detrimental due to causing pain, tissue damage, and infection, which makes patients reluctant to properly control their metabolic system. Therefore, the development of non-invasive methods needs to be further explored to provide a more comfortable alternative for biomarker management in diabetic patients (Gonzales et al., 2019; Susana et al., 2023).

Recent research indicates that  $\mu$ PADs (Microfluidic Paper-Based Analytical Devices) are POCT (Point-of-Care Testing) devices that offer ease in non-invasive detection. These devices are easy to fabricate, inexpensive, and versatile in their applications (Yu et al., 2020). In their development,  $\mu$ PADs have been broadly classified into two types of detection methods: distance-based detection and colorimetric detection. In terms of portability, the distance-based method is superior to the colorimetric method because it does not require additional analytical devices (Al-Jaf & Omer, 2023). In their application,  $\mu$ PADs have been successfully developed for the detection of glucose and ketone biomarkers in urine samples. However, the research conducted has been limited to the application of colorimetric detection and the role of enzymes. Although enzymes have high sensitivity, their stability only lasts under certain conditions, and their cost is less affordable (Taha et al., 2020; Mukhopadhyay et al., 2022). These weaknesses make  $\mu$ PADs less optimal for access in various regions with diverse stability conditions. To address this issue, the development of  $\mu$ PADs needs to employ other approaches that are enzyme-free but still provide high measurement sensitivity.

One such enzyme-free approach can be demonstrated through nanoscale interactions via the formation of nanoparticles (Fall et al., 2023; Hernández-Ramírez et al., 2022; Wu et al., 2023). Silver nanoparticles (AgNPs) have unique optical properties due to localized surface plasmon resonance (LSPR), which enables strong interactions with light. This capability can be utilized to create measurement systems that are sensitive to biomarkers (Loiseau et al., 2019). One interesting development is integrating  $\mu$ PADs with AgNPs as a portable detection system. In this research context, glucose is considered capable of acting as a reducing agent in the formation of AgNPs. This capability can be developed into a non-enzymatic glucose biomarker measurement method. The correlation between the amount of AgNPs formed and the concentration of glucose as a biomarker can be used as semi-quantitative measurement method. The quantification of glucose can

be assisted by sodium hydroxide, which acts as an accelerator in stimulating the reduction of  $\text{Ag}^+$  ions (Hemmati et al., 2019; Zhang et al., 2022). This approach can serve as an alternative to the use of glucose oxidase (GOx) in glucose detection, which is currently expensive and also sensitive to pH and temperature (Chen et al., 2020). Although this idea is innovative, the formation of AgNPs still faces challenges in overcoming nanoparticle agglomeration. Therefore, the use of capping agents is necessary in this research to control the size, reduction process, and stability of nanoparticles when integrated onto the paper substrate of  $\mu$ PADs. One capping agent that supports green chemistry is starch (Iqbal et al., 2020; Rather et al., 2019).

In addition to the nanoparticle approach, Schiff base reaction systems and the Rothera test are non-enzymatic methods capable of detecting ketones in the body, specifically acetoacetate ketones (Berber & Arslan, 2020; Mukhopadhyay et al., 2022). Both of these reactions are considered more effective for semi-quantitative testing compared to the commonly used ketometer. The ketometer has the drawback of relying on the enzyme  $\beta$ -hydroxybutyrate dehydrogenase to measure ketones (beta-hydroxybutyrate) in blood. While sensitive and specific, the ketometer has limitations in terms of invasive sample collection and the high cost of the enzyme (Crawford et al., 2024; Kausar et al., 2023). Therefore, the integration of Schiff base reaction systems and the Rothera test into  $\mu$ PADs presents a promising approach for ketone measurement. On the other hand, the development of  $\mu$ PADs-based detection systems utilizing capillary flow length faces challenges in controlling capillary fluid flow between the sample zone and the detection zone. These issues can lead to a decrease in detection resolution. To address this challenge, improving detection resolution is necessary by incorporating a 3D-connector. The addition of a 3D-connector can control unwanted reagent mixing between the fluids in the sample zone and the detection zone (Al-Jaf & Omer, 2022). The expected outcome of this research is to obtain a non-enzymatic measurement method simultaneously for glucose and ketone (acetoacetate) biomarkers through the design of a 3D- $\mu$ PADs (three-dimensional microfluidic paper-based analytical devices).

## Method

### *Materials and Tools*

The materials required for this research include Whatman No.1 chromatography paper from Cytiva (China), D-(+)-glucose anhydrous, starch, glycine ( $\geq 99.7\%$ ) obtained from Merck (Germany). Silver nitrate, sodium hydroxide, citric acid, sodium chloride obtained

from Emsure (Germany). Sodium nitroprusside (99.0%) obtained from Loba Chemie (India). Dimethylformamide (DMF) (99.8%), ethyl acetoacetate, acetone, sodium bicarbonate (99.5 – 100.5%), uric acid ( $\geq 99\%$ ), sodium sulfate decahydrate ( $\geq 99.0\%$ ), potassium dihydrogen phosphate ( $\geq 99.0\%$ ), dipotassium hydrogen phosphate ( $\geq 99.0\%$ ), ammonium chloride ( $\geq 99.5\%$ ), lactic acid ( $\geq 98\%$ ), calcium chloride dihydrate ( $\geq 99.0\%$ ), magnesium sulfate heptahydrate ( $\geq 99\%$ ), and urea obtained from Sigma Aldrich (Germany). The solvent used is distilled water.

The equipment needed during the research process includes a micropipette from Thermo Scientific (United States), glassware, vortex mixer, oven, hot plate, acrylic clamps, paper cutter, clear tape, Xerox ColorQube

8580DN Solid Ink Color printer, laptop with CorelDRAW Graphics Suite 2022 and ImageJ 1.54d software, a 25 MP smartphone camera, and a PULUZ Mini Studio Fotobox (camera-to-object distance: 15 cm).  
*Fabrication of 3D- $\mu$ PADs*

The 3D- $\mu$ PADs dual-channel design was created using CorelDraw Suite Graphics 2022 software. The design was printed on Whatman No.1 paper using the wax printing method with a Xerox ColorQube 8580DN Solid Ink Color printer. The printed paper was then heated in an oven at 120°C for 3 minutes to allow the wax to penetrate and form hydrophobic barriers. The wax-penetrated paper was then cut along the design boundaries. A simplified fabrication procedure scheme is shown in Figure 1.

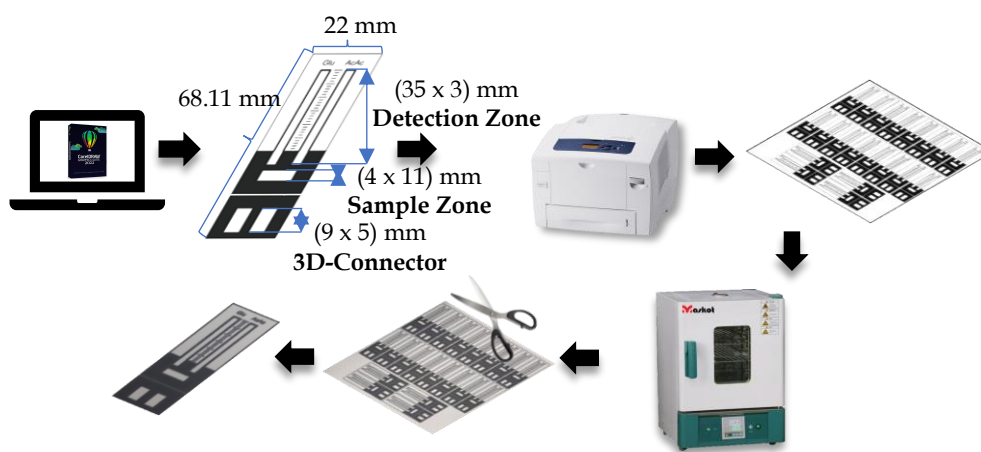


Figure 1. Scheme of 3D- $\mu$ PADs fabrication

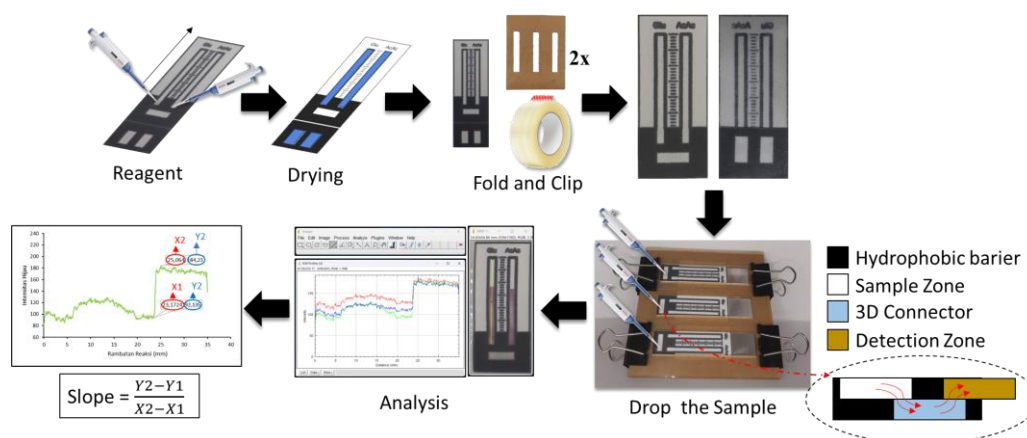


Figure 2. Procedure for simultaneous detection of glucose and acetoacetate with distance-based reaction analysis

*Analysis of Glucose and Acetoacetate Detection Distance Reaction*

The detection procedure was carried out by dispensing 10  $\mu$ L of a mixed solution of AgNO<sub>3</sub> 500 mM : starch 3%(w/v) in a (1:1) volume ratio from bottom to top on the glucose detection (Glu) zone. On the other

hand, the same treatment was done with a 900 mM glycine solution in 100 mM pH 9.4 phosphate buffer, dispensing 9  $\mu$ L on the acetoacetate detection (AcAc) zone. Next, a mixed solution of NaOH 10 M : starch 3% (w/v) in a (1:3) volume ratio was dispensed with 7  $\mu$ L on the Glucose detection (Glu) system's 3D-Connector.

On the other hand, a 15% (w/w) sodium nitroprusside solution in 5% (v/v) DMF was dispensed with 4.5  $\mu$ L on the Acetoacetate (AcAc) 3D-Connector. Then, the dispensed results were dried for 25 minutes at room temperature. The 3D-Connector was folded to connect the detection zone with the sample zone. The folded results were coated on the bottom part of the 3D- $\mu$ PADs with transparent tape. A standard solution of 8 mM glucose, 7 mM ethyl acetoacetate, and acetone in a volume ratio (1:1:1) in artificial urine was dispensed with 35  $\mu$ L on the sample zone. The dispensed results were allowed to stand for 5 minutes until color change reaction occurred at the detection zone. The intensity of the blue color slope was used for glucose detection ImageJ analysis, while the intensity of the green color slope was used for acetoacetate ketone detection ImageJ analysis. The scheme of the glucose and acetoacetate detection procedure up to the analysis of slope values can be shown in Figure 2.

*Method Validation*

The optimal conditions obtained from the optimization of reagent concentrations, volume variations, drying times, and reaction times were validated for method validation. The method validation included linearity, precision, accuracy, limit of detection (LOD), and limit of quantification (LOQ). The standard analyte solvent used was artificial urine with the composition shown in Table 1 (Hiraoka et al., 2020). Glucose detection linearity was assessed using standard analytes of 1, 2, 3, 5, 6, and 8 mM, while acetoacetate detection linearity was assessed using standard analytes of 1, 2, 3, 4, 5, and 7 mM. The precision test for both biomarkers was performed using high-concentration standard analytes. Precision was measured as the %RSD (% Relative Standard Deviation) of six replicate measurements of the standard analytes. The accuracy test was performed for standard analytes at each low, medium, and high concentration level. The sensitivity metrics LOD and LOQ were determined from the results of triplicate measurements of standard analytes on the linear curve.

**Table 1.** Composition of artificial urine

Components	Concentration (mM)
Citric acid	2
Urea	170
Uric acid	0.4
Lactic acid	1.1
Potassium dihydrogen phosphate	7
Dipotassium hydrogen phosphate	7
Sodium chloride	90
Sodium sulfate	10

Components	Concentration (mM)
Sodium bicarbonate	25
Ammonium chloride	25
Calcium chloride	2.5
Magnesium sulfate	2

*Research Workflow*

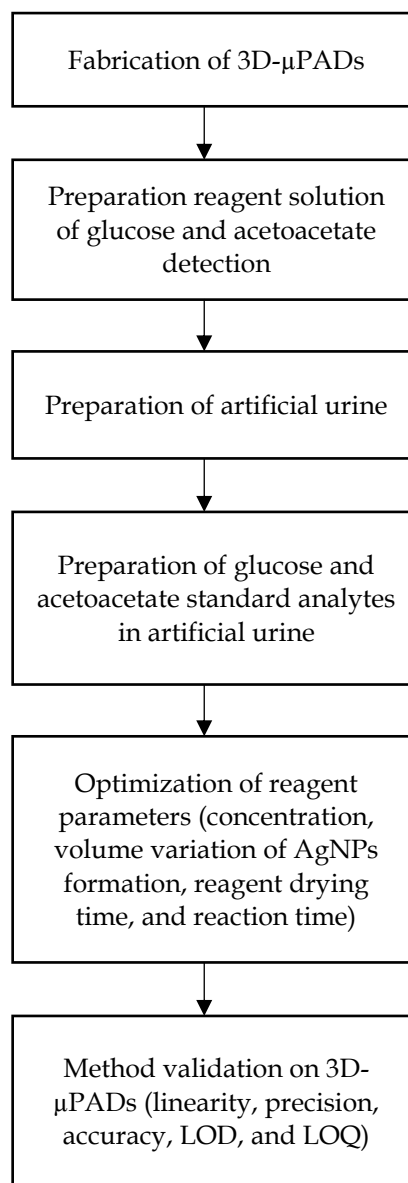


**Figure 3.** Research workflow

The research began with the fabrication of 3D- $\mu$ PADs using the wax printing method as shown in Figure 1. The design was applied with several pre-prepared glucose and ketone detection reagents. Each detection reagent solution was tested on standard analytes in artificial urine solvent. Before establishing the 3D- $\mu$ PADs measurement method, reagent parameter

optimization was necessary to determine optimal conditions that are easily observed during measurement. The optimal results from reagent parameter optimization were then applied in method validation to measure glucose and acetoacetate in urine. The research workflow can be simplified as shown in Figure 3.

## Result and Discussion

### The Influence of Analytes on the Detection System

Glucose detection in this study involves the analyte in an oxidized state. Oxidized glucose contributes to the formation of silver nanoparticles. The oxidized state of

glucose is indicated by the alkaline medium of sodium hydroxide. This condition occurs when the aldehyde group of glucose has electronegativity centered on the oxygen atom. This condition makes the carbon atom in the aldehyde group more likely to undergo nucleophilic addition. This nucleophilic addition process, which is commonly triggered by the presence of the OH<sup>-</sup> base ion, allows glucose to act as a carbanion. This carbanion can reduce Ag<sup>+</sup> ions from silver nitrate precursor to Ag<sup>0</sup> ions or AgNPs (El-Shishtawy et al., 2023). Previously oxidized glucose will be converted into gluconic acid. The process of glucose reducing Ag<sup>+</sup> ions can be shown according to Figure 4.

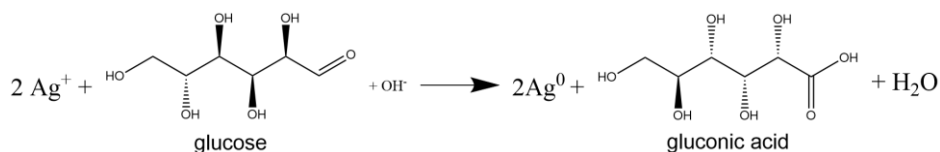


Figure 3. Reduction of silver ions (Ag<sup>+</sup>) by glucose to form AgNPs

Under these conditions, the reduced Ag<sup>0</sup> ions from Ag<sup>+</sup> do not stand alone, but rather combine with other Ag<sup>+</sup> ions to form Ag<sub>2</sub><sup>+</sup>. The combination of these two ions also undergoes dimerization again with Ag<sub>2</sub><sup>0</sup> to form Ag<sub>4</sub><sup>2+</sup>. Ag<sub>4</sub><sup>2+</sup> ions tend to be unstable, which makes the agglomeration of AgNPs a common occurrence. This is why these ions need to be controlled with more electronegative groups, such as the glycosidic bonds in starch. Starch, composed of amylose and amylopectin, has strong glycosidic bonds that can bind Ag<sub>4</sub><sup>2+</sup> ions, as shown in Figure 5 (Nguyen et al., 2022; Sanchez-Castañeda et al., 2020; Ponsanti et al., 2020). Under such conditions in AgNPs synthesis, a capping agent like starch is required to control the distribution of AgNPs on paper substrate.

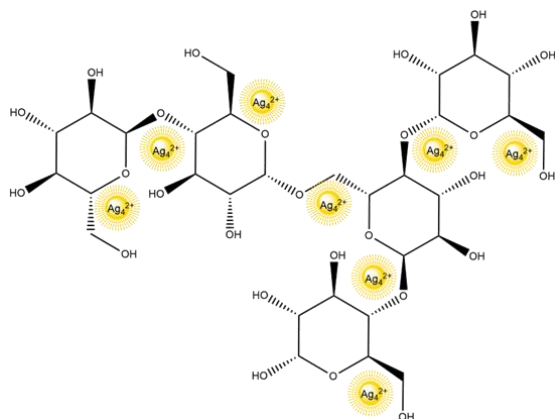


Figure 4. Silver nanoparticles bind to starch glycosidic bonds

On the other hand, acetoacetate detection involves the target analyte contributing to the formation of an imine derivative. This formation process occurs because acetoacetate has a ketone group on a secondary carbon atom. The position of the secondary carbon atom, which is more electrophilic, allows for the nucleophilic addition of the primary amine group of glycine. During the addition process, the primary amine group undergoes deprotonation and the formation of a double bond (C=N). Overall, the nucleophilic addition between primary amine condensation and the ketone group is known as the Schiff base reaction. The final product of this reaction is known by the specific term hemiaminal.

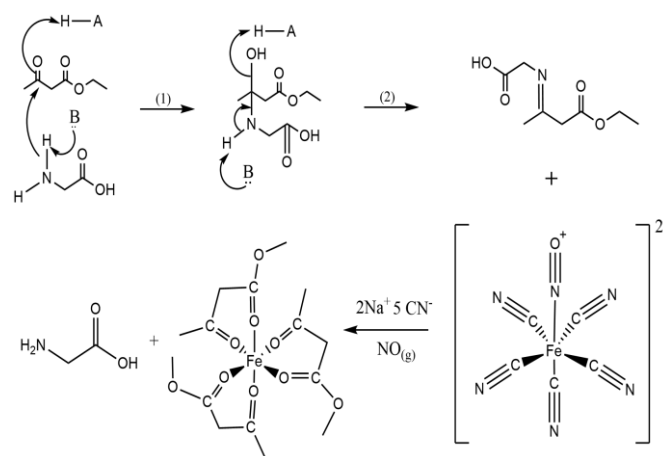


Figure 5. The reaction that occurs with the target analyte in acetoacetate detection

However, study cases show that the Schiff base reaction has problems when the reaction takes place under acidic pH conditions. The hemiaminal product tends not to form under acidic pH conditions because the abundance of  $H^+$  ions prevents the primary amine group from undergoing deprotonation. This necessitates the use of phosphate buffer solution pH 9.4 in these research. The failure of the primary amine group to undergo deprotonation can affect the nucleophilic addition reaction and the  $C=N$  bond cannot be formed. Hemiaminals have the characteristic of being ligands that can easily bind strongly to transition metals. Sodium nitroprusside itself has a central Fe atom that can easily bind to other ligands. This condition allows hemiaminal to form magenta complex (iron-acetate complex) when it reacts with sodium nitroprusside. The formation of an iron-acetate complex causes the cleavage of the  $(C=N)$  bond in the imine derivative, leading to the regeneration of glycine. The reaction mechanism of the target analyte in acetoacetate detection, which can form this complex, is shown in Figure 6 (Berber & Arslan, 2020; Poian & Castanho, 2021; Ibrahim & Abdalhadi, 2021).

*Effect of Reagent Concentration on AgNPs Formation*

Silver nitrate acts as an  $Ag^+$  ion precursor in the formation of AgNPs (Fu et al., 2021; Nguyen et al., 2023). The reduction of  $Ag^+$  ions from the precursor occurs at a specific concentration range to obtain AgNPs under optimal conditions. Optimal nanoparticles are those formed with uniform size, shape, and stability. This phenomenon is observed when 8 mM glucose in artificial urine is used to reduce  $Ag^+$  ions at a specific concentration variation on a paper substrate. According to this research study, analysis using ImageJ should show the optimal color range that can be observed by the eye due to its relationship in forming a measurement method. The results of ImageJ analysis show that the blue slope intensity value decreases at low concentrations, then increases optimally at a silver nitrate concentration of 500 mM, and decreases thereafter, as shown in Figure 7. Although low concentrations can provide higher slope values than 500 mM concentrations, this cannot be used as an optimal measurement standard because the color of the distance reaction tends to clump in the area near the 3D-Connector. Conversely, observations at concentrations above 300 mM show that the distance reaction starts to occur properly.

Glucose, without being oxidized in an alkaline medium, is unable to optimally reduce the silver nitrate precursor (Fahmi et al., 2024). This phenomenon can be observed when 8 mM glucose in artificial urine is used to reduce  $Ag^+$  ions on a paper substrate. ImageJ analysis

suggests that the optimal NaOH concentration is reached at a concentration of 10 M when the solubility limit occurs, as shown in Figure 8. The formation of optimal AgNPs is indicated by a yellow-brown color, and this condition is only observed at high concentrations. Conversely, at low concentrations, the blue slope intensity value tends to be low and the color of the distance reaction does not show yellow-brown. Low sodium hydroxide concentrations also result in a color range that is difficult to observe with the naked eye.

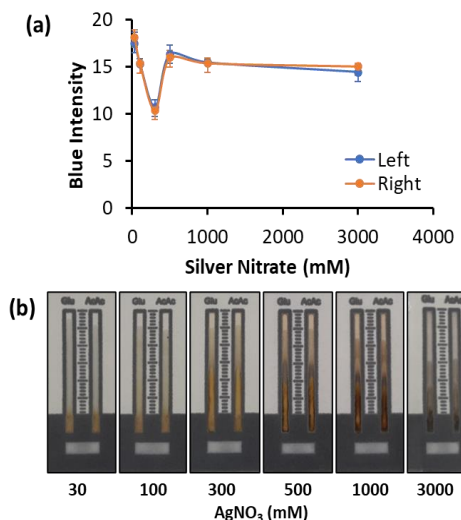


**Figure 6.** Influence of  $AgNO_3$  concentration on the blue slope intensity of distance reaction (a) and 3D- $\mu$ PADs images for  $AgNO_3$  reagent concentration optimization (b)

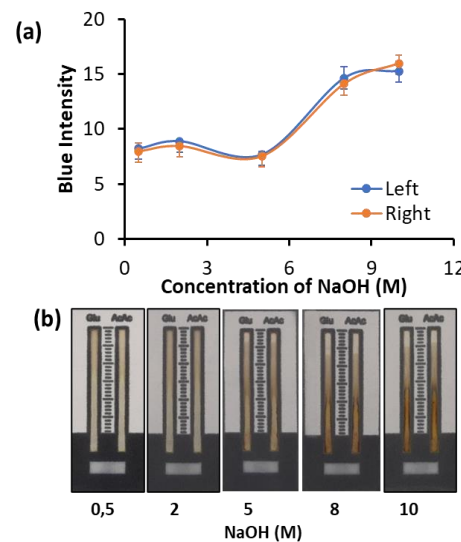


**Figure 7.** The influence of NaOH concentration on the blue slope intensity of distance reaction (a) and images for NaOH reagent concentration optimization (b)

Starch plays a crucial role in controlling the distribution of the formed nanoparticles. Synthesizing nanoparticles without the assistance of a capping agent like starch allows for uncontrolled nanoparticle aggregation, which can affect the color uniformity in the detection zone. This phenomenon can be observed through the analysis of the blue slope intensity values, as shown in Figure 9. The analysis results show that the slope value increases optimally up to a starch concentration of 3% (w/v) and then decreases above that concentration. This indicates that the optimal ability of 8 mM glucose to control the aggregation rate occurs when a 3% (w/v) starch concentration formula is applied to the paper substrate.

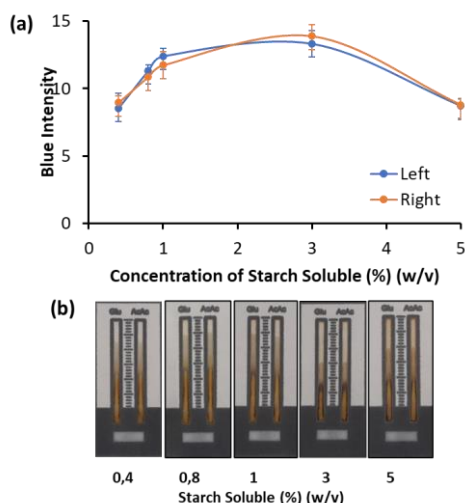


**Figure 8.** The influence of starch concentration on the blue slope intensity of distance reaction (a) and 3D-μPADs images for starch reagent concentration optimization (b)

*The Effect of Reagent Concentration on the Formation of Purple Complexes*

Glycine plays a role in the formation of imin derivatives or hemiaminals. The resulting product is converted into magenta complex. The increased amount of imin derivatives can indicate that the conversion of the amount of magenta complex formed is increasing. This phenomenon can be observed with 7 mM acetoacetate in artificial urine forming a magenta complex on a paper substrate. ImageJ analysis results show that the increase in the optimal green intensity slope value occurs at a concentration of 900 mM, and then the graph shows a decrease after that concentration, as shown in Figure 10. These conditions indicate that acetoacetate is able to optimally form a magenta complex when the glycine concentration is 900 mM.

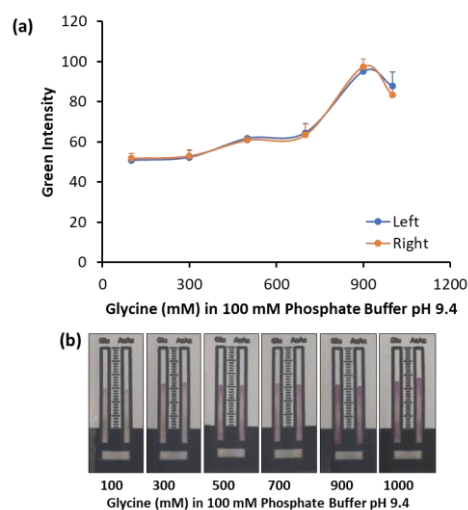


**Figure 9.** The influence of glycine concentration on the green slope intensity of distance reaction (a) and 3D-μPADs images for glycine reagent concentration optimization (b)

On the other hand, the influence of sodium nitroprusside is observed in playing a role in the conversion of imin derivatives to form a magenta complex. Under these conditions, the magenta complex formed should be obtained in line with the amount of imin derivative formed. This phenomenon is observed when 7 mM acetoacetate in artificial urine is used to form a magenta complex on a paper substrate. ImageJ analysis results according to Figure 11 show that the green intensity slope value increases up to a concentration of 15% (w/w) when solubility starts to become difficult. This condition indicates that 7 mM acetoacetate in artificial urine is effectively able to form a magenta complex only at a concentration of 15% (w/w).

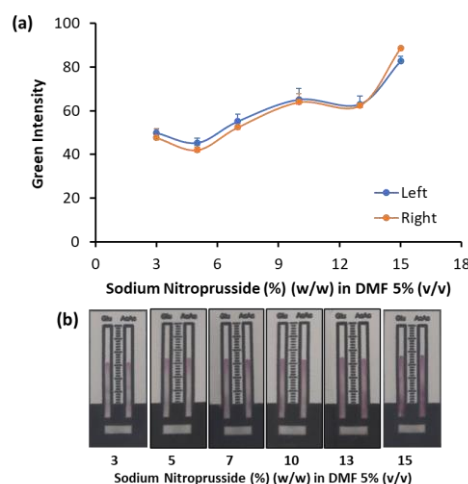


**Figure 10.** The influence of sodium nitroprusside concentration on the green slope intensity of distance reaction (a) and 3D-μPADs images for nitroprusside reagent concentration optimization (b)

*The Effect of Reagent Volume Variation on the Formation of AgNPs*

The effect of variations in the  $\text{AgNO}_3$  to starch volume ratio has an influence on the color of the distance reaction in the detection zone. An insufficient amount of starch volume in the detection zone reagent formula affects the uneven distribution of AgNPs color. The phenomenon of the effect of starch volume variation is observed through the analysis of the blue intensity slope, as shown in Figure 12. The graph increases optimally at a volume ratio of 1:1, then the graph decreases after passing through the volume ratio formula. These results indicate that increasing the volume of starch does not provide an optimal control value for the even distribution of AgNPs in the detection zone. Conversely, the absence of starch volume in the detection zone shows color aggregation in some parts of the detection zone. In this condition, excessive starch increases the solution's viscosity, making it difficult to handle and unsuitable for further study. This occurs because starch, as a complex polymer, forms denser networks at higher concentrations, disrupting the interaction between  $\text{AgNO}_3$  and starch essential for the reduction process and AgNP formation (Tarmizi et al., 2022).

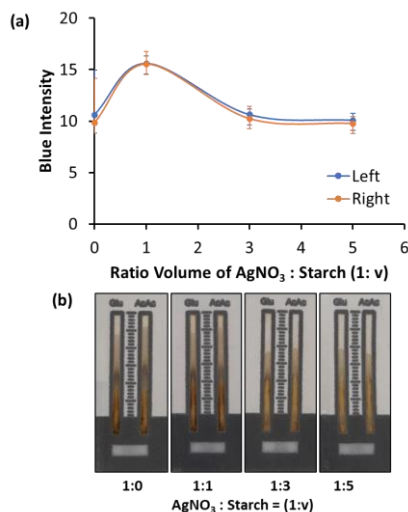


**Figure 11.** The influence of volume ratio  $\text{AgNO}_3$  to starch (1:v) on the detection zone (a) and 3D- $\mu$ PADs image for  $\text{AgNO}_3$  to starch volume ratio optimization (b)

The effect of starch volume variations in the 3D-Connector is evident beyond the detection zone. An excessive NaOH volume causes bends in the 3D-Connector, as shown in Figure 13, making folding difficult and disrupting the alignment of reaction rates between the two channels in the detection zone. This suggests that the starch volume not only influences AgNP formation in the detection zone but also impacts

glucose oxidation in the 3D-Connector. Observations in Figure 13 indicate that an optimal NaOH-to-starch ratio of 1:3 minimizes these issues. Excessive starch reduces glucose oxidation by hydroxide ions ( $\text{OH}^-$ ), while suboptimal ratios degrade cellulose chains in paper (Sayakulu & Soloi, 2022). Careful optimization of the NaOH and starch formulation is therefore crucial to ensure the 3D-Connector performance.

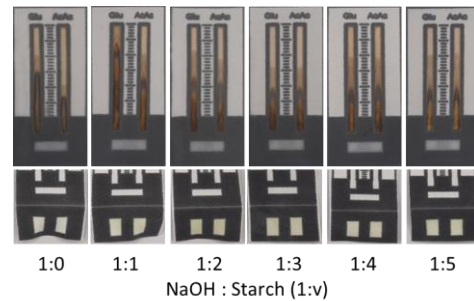


**Figure 12.** The influence of NaOH to starch volume ratio (1:v) on the 3D-Connector

*The Effect of Drying Time*

The drying time has an influence on the formation of the distance reaction color in the detection zone (Fahmi et al., 2024). Longer drying times can increase the concentration of fluid in the detection zone. The more concentrated fluid is able to provide optimal reaction color in the detection zone. The formation of optimal color can facilitate observation and measurement with the naked eye. ImageJ analysis shows that the slope color intensity value for glucose and acetoacetate detection increases optimally at a drying time of 25 minutes, then the slope value decreases after that time, as shown in Figure 14.

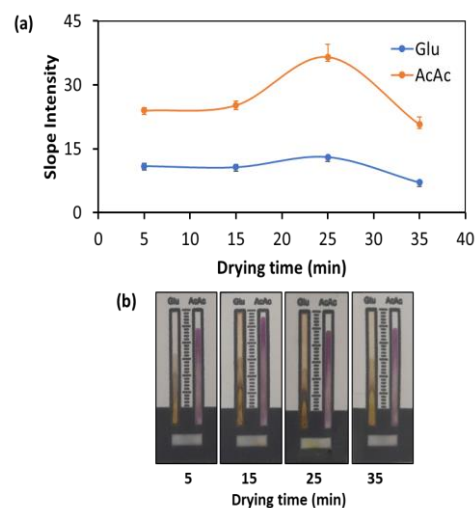


**Figure 13.** The influence of drying time on the slope intensity of distance reaction (a) and 3D- $\mu$ PADs image for drying time optimization (b)

The Effect of Reaction Time

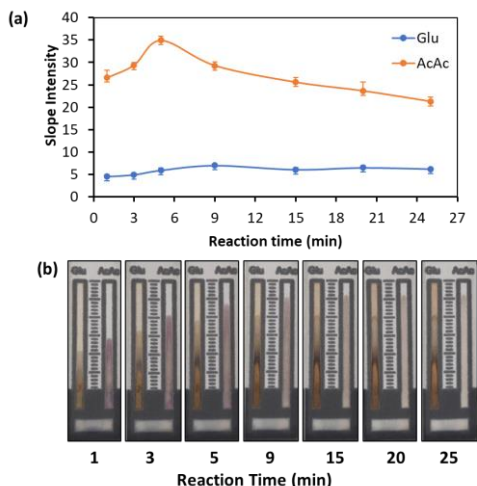


Figure 14. The influence of reaction time on the slope intensity of distance reaction (a) and 3D-μPADs image for reaction time optimization (b)

Method Validation

Table 2. Accuracy test results for standard analytes at three scale concentrations

Glucose Concentration in Artificial Urine (mM)	Distance Reaction (n = 3)	Measured Concentration	Acetoacetate Concentration in Artificial Urine (mM)	Distance Reaction (n = 3)	Measured Concentration
1.5	7.33 ± 0.58	1.67 ± 1.00 (11.26 %)	1.5	27.33 ± 0.60	1.50 ± 0.60 (0.27 %)
4	8.67 ± 0.58	3.99 ± 1.00 (0.38 %)	3.5	29.33 ± 0.60	3.59 ± 0.60 (2.56 %)
7	10.33 ± 0.58	6.88 ± 1.00 (1.72 %)	6	31.67 ± 0.60	6.02 ± 0.60 (0.38 %)

\*The numbers in parentheses indicate the measurement error

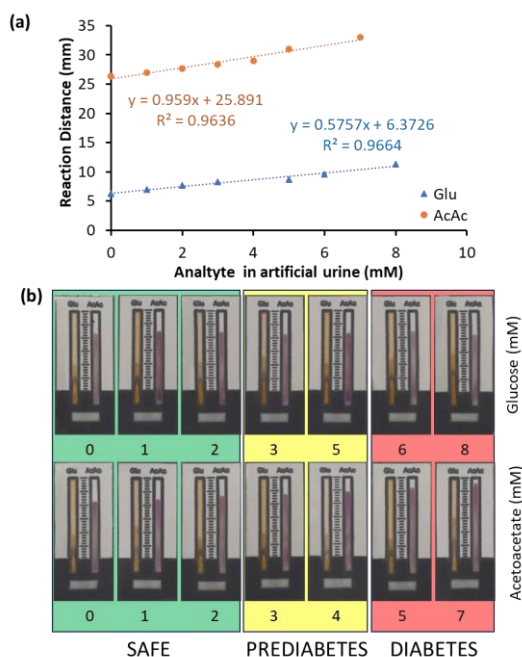


Figure 15. Analytical measurement of the linearity standard for glucose (Glu) and acetoacetate (AcAc) (a) detection and the 3D-μPADs observation images (b)

The reaction time significantly impacts the analyte's ability to convert precursors into AgNPs and magenta complexes. The optimal reaction time is achieved when both detection systems facilitate the observation of distance reaction with the naked eye. ImageJ analysis reveals that the distance reaction for both glucose and acetoacetate detection occurs at distinct times, as depicted in Figure 15. The slope intensity value of the glucose detection system exhibits an optimal peak at 9 minutes. In contrast, the slope intensity of acetoacetate detection reaches an optimal value at 5 minutes. This observation indicates that the optimal reaction time for both reactions is 5 minutes. The determination of this optimal reaction time is based on preventing a decrease in the optimal color limit of the acetoacetate detection system during simultaneous measurements.

Several optimized parameters were then applied to the linearity standard curve of the measurement. Linearity plays a crucial role in demonstrating the correlation between distance reaction color on the y-axis and the analyte present in artificial urine on the x-axis. In the glucose detection system, the oxidized analyte is expected to reduce  $Ag^+$  ions in line with the number of nanoparticles formed. Conversely, in the acetoacetate detection system, the analyte is expected to exhibit the formation of a magenta complex. The obtained linearity can be observed in Figure 16. A comparison of the two standard curves between the glucose detection system and the acetoacetate detection system reveals that the coefficient of determination value for glucose measurement ( $R^2 = 0.9664$ ) is higher than the coefficient of determination value for acetoacetate measurement ( $R^2 = 0.9636$ ).

Precision testing of repeated measurements was conducted for high-concentration glucose and acetoacetate analytes. The precision test with six replications is depicted in Figure 17. Six-replicate measurements of 8 mM glucose in artificial urine revealed two inconsistent data points. The RSD for these

glucose measurements was 4.56%, significantly higher than that for acetoacetate measurements. Six-replicate measurements of 7 mM acetoacetate in artificial urine revealed one inconsistent data point. The RSD for these acetoacetate measurements was 1.24%.

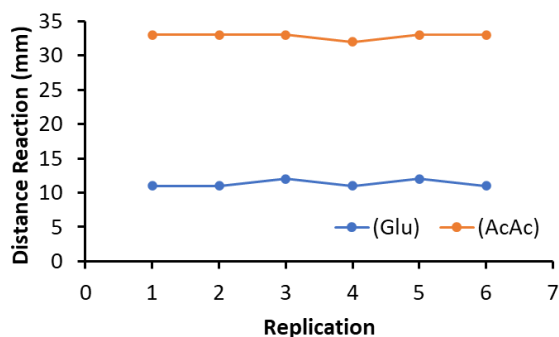


**Figure 16.** Precision testing of standard analyte measurements

Accuracy testing of the two detection systems was performed in triplicate for each low, medium, and high concentration. The measurement accuracy results are presented in Table 2. The accuracy test results for glucose detection indicate that the highest measurement error occurs at the low concentration, with a value of 11.26%. In contrast, for medium and high glucose concentrations, the error difference can be obtained below 2%. On the other hand, the acetoacetate detection system was able to provide accuracy testing with an error rate below 3%. The highest measurement error in the acetoacetate detection system was obtained at the medium concentration with an error difference of 2.56%.

The 3D- $\mu$ PADs dual-channel detection system was also used to determine the lowest limit of detection (LOD) and limit of quantification (LOQ) for the analyte samples. Measurements were performed in triplicate, and the glucose detection system demonstrated capabilities of (LOD = 1.61 mM) and (LOQ = 5.37 mM). On the other hand, measurements with the acetoacetate detection system resulted in capabilities of (LOD = 1.41 mM) and (LOQ = 4.69 mM). These results indicate that the glucose and acetoacetate detection systems developed in this study are effective for measuring high-concentration biomarkers.

## Conclusion

A novel non-enzymatic detection method for diagnosing glycosuria and ketonuria has been developed, providing an alternative approach to measuring analyte levels. The glucose detection system was developed using an AgNPs synthesis approach, while the acetoacetate detection system was developed using Schiff base synthesis and the Rothera test. The

detection system was also developed by combining simultaneous measurement detection and the addition of a 3D-Connector. The 3D-Connector was chosen because it can improve detection resolution by controlling unwanted reagent mixing between the sample zone and the detection zone. Optimal conditions were obtained as follows: the glucose detection zone was occupied by a combination of AgNO<sub>3</sub> : starch volume ratio (1 : 1), the acetoacetate detection zone was occupied by 900 mM glycine in 100 mM phosphate buffer pH 9.4, and the sample zone was occupied by a combination of glucose, acetoacetate, and acetone in artificial urine with a volume ratio of (1 : 1 : 1). The glucose 3D-Connector was occupied by a combination of NaOH : starch volume ratio (1 : 3), and the acetoacetate 3D-Connector was occupied by 15% (w/w) sodium nitroprusside in 5% DMF solvent. The method validation obtained for glucose measurement is as follows: linearity ( $R^2 = 0.9664$ ), precision test (RSD = 4.56%), accuracy test (88.75 - 99.62%), LOD (1.61 mM), and LOQ (5.37 mM). The method validation obtained for acetoacetate measurement is as follows: linearity ( $R^2 = 0.9636$ ), precision test (RSD = 1.24%), accuracy test (99.44 - 99.73%), LOD (1.41 mM), and LOQ (4.69 mM).

## Acknowledgments

We would like to thank Institute of Research and Community Services Brawijaya University (LPMM) Brawijaya University for the financial support and Brawijaya University Facilitating this work.

## Author Contributions

A.L.F. and K.R.A. conducted experiments and data analysis, wrote the original manuscript, and revised the manuscript. I.O.W. and H.S. formulated the idea, supervised the project, and revised the manuscript. A.S. formulated the idea, provided funding, supervised the project, and revised the manuscript. All authors approved the final version of the manuscript.

## Funding

This research was funded by the Institute of Research and Community Services Brawijaya University (LPMM) through the 2024 Research Ecosystem Strengthening Grant.

## Conflicts of Interest

The authors have no conflict of interest.

## References

- Al-Jaf, S. H., & Omer, K. M. (2022). Enhancing of Detection Resolution Via Designing of a Multi-Functional 3D Connector between Sampling and Detection Zones in Distance-Based Microfluidic Paper-Based Analytical Device: Multi-Channel Design for Multiplex Analysis. *Microchimica Acta*, 189(482), 1-10. [https://doi.org/10.1007/s00604-](https://doi.org/10.1007/s00604-189(482), 1-10)

- 022-05585-y
- Al-Jaf, S. H., & Omer, K. M. (2023). Accuracy Improvement Via Novel Ratiometry Design in Distance-Based Microfluidic Paper Based Analytical Device: Instrument-Free Point of Care Testing. *RSC Advances*, 13(23), 15704–15713. <https://doi.org/10.1039/d3ra01601c>
- Berber, N., & Arslan, M. (2020). Preparation and Characterization of Some Schiff Base Compounds. *Adiyaman University Journal of Science*, 10(1), 179–188. <https://doi.org/10.37094/adyujsci.633080>
- Chen, Z., Wright, C., Dincel, O., Chi, T. Y., & Kameoka, J. (2020). A Low-Cost Paper Glucose Sensor with Molecularly Imprinted Polyaniline Electrode. *Sensors (Switzerland)*, 20(4), 1–11. <https://doi.org/10.3390/s20041098>
- Crawford, S. G., Coker, R. H., & Rea, L. D. (2024). Preliminary Comparisons between a Point-of-Care Ketometer and Reference Method Using Steller Sea Lion Pup Whole Blood and Plasma. *Conservation Physiology*, 12(1), 1–10. <https://doi.org/10.1093/conphys/coad104>
- El-Shishtawy, R. M., Angari, Y. M. A., Alotaibi, M. M., & Almulaiky, Y. Q. (2023). Novel and Facile Colorimetric Detection of Reducing Sugars in Foods Via In Situ Formed Gelatin-Capped Silver Nanoparticles. *Polymers*, 15(5), 1–13. <https://doi.org/10.3390/polym15051086>
- Fahmi, A. L., 'Aisy, K. R., Wulandari, I. O., Sulistyarti, H., & Sabarudin, A. (2024). Non-Enzymatic Determination of Glucose in Artificial Urine Using 3D- $\mu$ PADs Through Silver Nanoparticles Formation. *Indonesian Journal of Chemistry*, 24(5), 1481. <https://doi.org/10.22146/ijc.95588>
- Fall, B., Sall, D. D., Hémadi, M., Diaw, A. K. D., Fall, M., Randriamahazaka, H., & Thomas, S. (2023). Highly Efficient Non-Enzymatic Electrochemical Glucose Sensor Based on Carbon Nanotubes Functionalized by Molybdenum Disulfide and Decorated with Nickel Nanoparticles (GCE/CNT/MoS<sub>2</sub>/NiNPs). *Sensors and Actuators Reports*, 5, 1–11. <https://doi.org/10.1016/j.snr.2022.100136>
- Fu, L.-M., Hsu, J.-H., Shih, M.-K., Hsieh, C.-W., Ju, W.-J., Chen, Y.-W., Lee, B. H., & Hou, C.-Y. (2021). Process Optimization of Silver Nanoparticle Synthesis and Its Application in Mercury Detection. *Micromachines*, 12(9), 1–16. <https://doi.org/10.3390/mi12091123>
- Galicia-Garcia, U., Benito-Vicente, A., Jebari, S., Larrea-Sebal, A., Siddiqi, H., Uribe, K. B., Ostolaza, H., & Martín, C. (2020). Pathophysiology of Type 2 Diabetes Mellitus. *International Journal of Molecular Sciences*, 21(17), 1–34. <https://doi.org/10.3390/ijms21176275>
- Gonzales, W. V., Mobashsher, A. T., & Abbosh, A. (2019). The Progress of Glucose Monitoring – A Review of Invasive to Minimally and Non-Invasive Techniques, Devices and Sensors. *Sensors (Switzerland)*, 19, 1–45. <https://doi.org/10.3390/s19040800>
- Hassan, E. M., Mushtaq, H., Mahmoud, E. E., Chhibber, S., Saleem, S., Issa, A., Nitesh, J., Jama, A. B., Khedr, A., Boike, S., Mir, M., Attallah, N., Surani, S., & Khan, S. A. (2022). Overlap of Diabetic Ketoacidosis and Hyperosmolar Hyperglycemic State. *World Journal of Clinical Cases*, 10(32), 11702–11711. <https://doi.org/10.12998/wjcc.v10.i32.11702>
- Hemmati, S., Retzlaff-Roberts, E., Scott, C., & Harris, M. T. (2019). Artificial Sweeteners and Sugar Ingredients as Reducing Agent for Green Synthesis of Silver Nanoparticles. *Journal of Nanomaterials*, 2019, 1–16. <https://doi.org/10.1155/2019/9641860>
- Hernández-Ramírez, D., Mendoza-Huizar, L. H., Galán-Vidal, C. A., Aguilar-Lira, G. Y., & Álvarez-Romero, G. A. (2022). Development of a Non-Enzymatic Glucose Sensor Based on Fe<sub>2</sub>O<sub>3</sub> Nanoparticles-Carbon Paste Electrodes. *Journal of The Electrochemical Society*, 169(6), 1–7. <https://doi.org/10.1149/1945-7111/ac735c>
- Hillock, M. F., Jarmon, C., Metropulos, A. E., King, R., Tchernodriniski, S., & Principe, D. R. (2024). Diabetic Ketoacidosis Masked by Both Euglycemia and a Primary Metabolic Alkalosis. *Oxford Medical Case Reports*, 2024(7), 288–290. <https://doi.org/10.1093/omcr/omae071>
- Hiraoka, R., Kuwahara, K., Wen, Y.-C., Yen, T.-H., Hiruta, Y., Cheng, C.-M., & Citterio, D. (2020). Paper-Based Device for Naked Eye Urinary Albumin/Creatinine Ratio Evaluation. *ACS Sensors*, 5(4), 1110–1118. <https://doi.org/10.1021/acssensors.0c00050>
- Ibrahim, F. M., & Abdalhadi, S. M. (2021). Performance of Schiff Bases Metal Complexes and Their Ligand in Biological Activity: A Review. *Al-Nahrain Journal of Science*, 24(1), 1–10. <https://doi.org/10.22401/ANJS.24.1.01>
- Iqbal, M., Zafar, H., Mahmood, A., Niazi, M. B. K., & Aslam, M. W. (2020). Starch-Capped Silver Nanoparticles Impregnated Into Propylamine-Substituted PVA Films with Improved Antibacterial and Mechanical Properties for Wound-Bandage Applications. *Polymers*, 12(9), 1–17. <https://doi.org/10.3390/POLYM12092112>
- Kausar, F., Sarwar, M., Aslam, A., Jamil, A., Sultana, N., & Shaffqat, G. (2023). Role of Capillary Blood Ketone Assay in Management of Diabetic Ketoacidosis in Paediatric Intensive Care Unit. *Pakistan Armed Forces Medical Journal*, 73(5), 1448–

1451. <https://doi.org/10.51253/pafmj.v73i5.9116>
- Loiseau, A., Asila, V., Boitel-Aullen, G., Lam, M., Salmain, M., & Boujday, S. (2019). Silver-Based Plasmonic Nanoparticles for and Their Use in Biosensing. *Biosensors*, 9(2), 1–39. <https://doi.org/10.3390/bios9020078>
- Mukhopadhyay, M., Subramanian, S. G., Durga, K. V., Sarkar, D., & DasGupta, S. (2022). Laser Printing Based Colorimetric Paper Sensors for Glucose and Ketone Detection: Design, Fabrication, and Theoretical Analysis. *Sensors and Actuators B: Chemical*, 371, 1–10. <https://doi.org/10.1016/j.snb.2022.132599>
- Nasser, S., Vialichka, V., Biesiekierska, M., Balcerczyk, A., & Pirola, L. (2020). Effects of Ketogenic Diet and Ketone Bodies on the Cardiovascular System: Concentration Matters. *World Journal of Diabetes*, 11(12), 584–595. <https://doi.org/10.4239/wjd.v11.i12.584>
- Nguyen, H. T., Nguyen, T. D., Nguyen, D. P., Thai, N. T. T., & Nguyen, T. H. (2022). Synthesis Efficiency of Silver Nanoparticles by Light-Emitting Diode and Microwave Irradiation Using Starch as a Reducing Agent. *Nanotechnology for Environmental Engineering*, 7(1), 297–306. <https://doi.org/10.1007/s41204-022-00231-7>
- Nguyen, N. P. U., Dang, N. T., Doan, L., & Nguyen, T. T. H. (2023). Synthesis of Silver Nanoparticles: From Conventional to 'Modern' Methods – A Review. *Processes*, 11(9), 1–17. <https://doi.org/10.3390/pr11092617>
- Poian, A. T. D., & Castanho, M. A. R. B. (2021). Integrative Human Biochemistry. In *Integrative Human Biochemistry*. Cham: Springer International Publishing.
- Ponsanti, K., Tangnorawich, B., Ngernyuang, N., & Pechyen, C. (2020). A Flower Shape-Green Synthesis and Characterization of Silver Nanoparticles (AgNPs) with Different Starch as a Reducing Agent. *Journal of Materials Research and Technology*, 9(5), 11003–11012. <https://doi.org/10.1016/j.jmrt.2020.07.077>
- Ramteke, P., Deb, A., Shepal, V., & Bhat, M. K. (2019). Hyperglycemia Associated Metabolic and Molecular Alterations in Cancer Risk, Progression, Treatment, and Mortality. *Cancers*, 11(9), 1–23. <https://doi.org/10.3390/cancers11091402>
- Rather, R. A., Sarwara, R. K., Das, N., & Pal, B. (2019). Impact of Reducing and Capping Agents on Carbohydrates for the Growth of Ag and Cu Nanostructures and Their Antibacterial Activities. *Particuology*, 43, 219–226. <https://doi.org/10.1016/j.partic.2018.01.004>
- Sanchez-Castañeda, M. P., Cañon-Ibarra, A. F., Cruz-Posada, A. F., Sanchez, L. T., Pinzon, M. I., & Villa, C. C. (2020). Synthesis and Characterization of Starch Stabilized Ag Nanoparticles Effect of the Crystalline Structure of Starch. *Journal of Physics: Conference Series*, 1541(1), 1–6. <https://doi.org/10.1088/1742-6596/1541/1/012003>
- Sayakulu, N. F., & Soloi, S. (2022). The Effect of Sodium Hydroxide (NaOH) Concentration on Oil Palm Empty Fruit Bunch (OPEFB) Cellulose Yield. *Journal of Physics: Conference Series*, 2314(1), 012017. <https://doi.org/10.1088/1742-6596/2314/1/012017>
- Susana, E., Ramli, K., Purnamasari, P. D., & Apriantoro, N. H. (2023). Non-Invasive Classification of Blood Glucose Level Based on Photoplethysmography Using Time-Frequency Analysis. *Information (Switzerland)*, 14(3), 1–18. <https://doi.org/10.3390/info14030145>
- Taha, M. F., Ashraf, H., & Caesarendra, W. (2020). A Brief Description of Cyclic Voltammetry Transducer-Based Non-Enzymatic Glucose Biosensor Using Synthesized Graphene Electrodes. *Applied System Innovation*, 3(3), 1–33. <https://doi.org/10.3390/asi3030032>
- Tarmizi, Z. I., Burhanuddin, M. F. B., Shahrul, M., Mokhtar, M. A. M., Zhe, J. C., Taib, S. H. M., & Sukri, S. N. A. (2022). Preparation and Characterization of Acetylated Starch Mediated Silver Nanoparticles: The Effect of Solution Ratio and Time-Varying Exposure. *Journal of Physics: Conference Series*, 2259(1), 012005. <https://doi.org/10.1088/1742-6596/2259/1/012005>
- Wu, B., Xue, Q., Fan, Y., Cui, D., Sun, Y., Xu, B. B., Wei, H., Li, H., Wasnik, P., Sridhar, D., Algadi, H., Guo, Z., & Annamareddy, S. H. K. (2023). Multifunctional Polymer Nanocomposites for Non-Enzymatic Glucose Detection: A Brief Review. *ES Food & Agroforestry*, 12, 1–11. <https://doi.org/10.30919/esfaf859>
- Yu, P., Deng, M., Yang, Y., Nie, B., & Zhao, S. (2020). 3D Microfluidic Devices in a Single Piece of Paper for the Simultaneous Determination of Nitrite and Thiocyanate. *Sensors (Switzerland)*, 20(15), 1–15. <https://doi.org/10.3390/s20154118>
- Zhang, Z., Yang, G., He, M., Qi, L., Li, X., & Chen, J. (2022). Synthesis of Silver Nanoparticles and Detection of Glucose via Chemical Reduction with Nanocellulose as Carrier and Stabilizer. *International Journal of Molecular Sciences*, 23(23), 1–13. <https://doi.org/10.3390/ijms232315345>